



DRACULA2 is a dynamic nucleoporin with a role in regulating the shade avoidance syndrome in Arabidopsis

Marçal Gallemi, Anahit Galstyan, Sandi Paulisic, Christiane Then, Almudena Ferrandez-Ayela, Laura Lorenzo-Orts, Irma Roig-Villanova, Xuewen Wang, Jose Luis Micol, Maria Rosa Ponce, et al.

► To cite this version:

Marçal Gallemi, Anahit Galstyan, Sandi Paulisic, Christiane Then, Almudena Ferrandez-Ayela, et al.. DRACULA2 is a dynamic nucleoporin with a role in regulating the shade avoidance syndrome in Arabidopsis. *Development* (Cambridge, England), 2016, 143 (9), pp.1623-1631. 10.1242/dev.130211 . hal-01607742

HAL Id: hal-01607742

<https://hal.science/hal-01607742>

Submitted on 27 May 2020

HAL is a multi-disciplinary open access archive for the deposit and dissemination of scientific research documents, whether they are published or not. The documents may come from teaching and research institutions in France or abroad, or from public or private research centers.

L'archive ouverte pluridisciplinaire **HAL**, est destinée au dépôt et à la diffusion de documents scientifiques de niveau recherche, publiés ou non, émanant des établissements d'enseignement et de recherche français ou étrangers, des laboratoires publics ou privés.

RESEARCH ARTICLE

DRACULA2 is a dynamic nucleoporin with a role in regulating the shade avoidance syndrome in *Arabidopsis*

Marçal Gallemí^{1,*,**}, Anahit Galstyan^{1,‡,**}, Sandi Paulišić¹, Christiane Then^{1,§}, Almudena Ferrández-Ayela², Laura Lorenzo-Orts¹, Irma Roig-Villanova¹, Xuewen Wang^{3,¶}, Jose Luis Micol², Maria Rosa Ponce², Paul F. Devlin³ and Jaime F. Martínez-García^{1,4,‡†}

ABSTRACT

When plants grow in close proximity basic resources such as light can become limiting. Under such conditions plants respond to anticipate and/or adapt to the light shortage, a process known as the shade avoidance syndrome (SAS). Following genetic screening using a shade-responsive luciferase reporter line (PHYB:LUC), we identified *DRACULA2* (*DRA2*), which encodes an *Arabidopsis* homolog of mammalian nucleoporin 98, a component of the nuclear pore complex (NPC). *DRA2*, together with other nucleoporins, participates positively in the control of the hypocotyl elongation response to plant proximity, a role that can be considered dependent on the nucleocytoplasmic transport of macromolecules (i.e. is transport dependent). In addition, our results reveal a specific role for *DRA2* in controlling shade-induced gene expression. We suggest that this novel regulatory role of *DRA2* is transport independent and that it might rely on its dynamic localization within and outside of the NPC. These results provide mechanistic insights in to how SAS responses are rapidly established by light conditions. They also indicate that nucleoporins have an active role in plant signaling.

KEY WORDS: *Arabidopsis thaliana*, Nucleoporin, Nup98, Hypocotyl elongation, Shade avoidance syndrome, Shade-induced gene expression

INTRODUCTION

As sessile organisms, plants cannot move to the best places to grow: therefore, they either adapt or die. One unfavorable situation is to grow in crowded conditions (e.g. those found in forests, prairies or agricultural communities), since the close proximity of neighboring plants can result in competition for limited resources, such as light. The shade avoidance syndrome (SAS) comprises the set of plant responses aimed to adapt growth and development to high plant density environments. Neighboring plants selectively absorb red light (R) and reflect far-red light (FR), resulting in a moderate

reduction in the R to FR ratio (R:FR). Under plant canopy shade, the concomitant reduction in light intensities results in even lower R:FR ratios. In either case, these changes become a signal perceived by the R- and FR-absorbing phytochrome photoreceptors (Smith, 1982; Smith and Whitelam, 1997; Keuskamp et al., 2010; Martínez-García et al., 2010).

In *Arabidopsis thaliana* (hereafter *Arabidopsis*), a gene family of five members (*PHYA-PHYE*) encodes the phytochromes (Bae and Choi, 2008), which have positive (phyB-phyE) and negative (phyA) roles in controlling SAS-driven development (Franklin, 2008; Martínez-García et al., 2010, 2014). Phytochromes exist in two photoconvertible forms: an inactive R-absorbing Pr form and an active FR-absorbing Pfr form. Under sunlight (i.e. a high R:FR ratio), the photo-equilibrium is displaced towards the active Pfr forms, and SAS is suppressed. Under a low R:FR ratio, the phytochrome photo-equilibrium is displaced towards the inactive Pr forms, and SAS is induced by affecting the interaction with PHYTOCHROME INTERACTING FACTORS (PIFs) and altering their stability and/or activity (Smith and Whitelam, 1997; Martínez-García et al., 2000; Lorrain et al., 2008; Leivar and Quail, 2011), which results in rapid changes in the expression of dozens of *PHYTOCHROME RAPIDLY REGULATED* (*PAR*) genes (Salter et al., 2003; Roig-Villanova et al., 2006, 2007; Lorrain et al., 2008). Because most of these *PAR* genes encode transcriptional regulators, it is assumed that SAS responses are a consequence of the regulation of a complex transcriptional network by phytochromes (Bou-Torrent et al., 2008; Josse et al., 2008). Indeed, genetic approaches have demonstrated regulatory roles in SAS for a large number of *PAR* genes encoding transcriptional regulators, including members of at least three different families: basic helix-loop-helix (HFR1, PAR1, PAR2, BIMs and BEEs), homeodomain-leucine zipper (HD-ZIP) class II (ATHB2, ATHB4, HAT1, HAT2 and HAT3), and B-BOX-CONTAINING (BBX). PIF stability and/or activity was also shown to be increased by low R:FR perception (Lorrain et al., 2008; Li et al., 2012). Genetic analyses unraveled roles for these factors in the negative (including BBX21, BBX22, HFR1, PAR1, PAR2 and PIL1) or positive (including BBX24, BBX25, PIFs, BIMs and BEEs) regulation of SAS (Sessa et al., 2005; Roig-Villanova et al., 2006, 2007; Crocco et al., 2010; Cifuentes-Eskivel et al., 2013; Gangappa et al., 2013; Bou-Torrent et al., 2015). Therefore, the low R:FR perception rapidly changes the balance of positive and negative factors, resulting in the appropriate SAS responses.

Phytochromes are known to partition between the cytoplasm and nucleus (and even within the nucleus) in a light-dependent manner; similarly, after low R:FR exposure, newly formed and shade-stabilized PIFs rapidly reach the nucleus. To do so these proteins have to cross the nuclear envelope, a physical barrier that separates both cell compartments. The nuclear pore complex (NPC) is a large multiprotein complex that is the sole gateway of macromolecular

¹Centre for Research in Agricultural Genomics (CRAG), CSIC-IRTA-UAB-UB, Campus UAB, 08193 Barcelona, Spain. ²Instituto de Bioingeniería, Universidad Miguel Hernández, Campus de Elche, 03202 Elche, Spain. ³School of Biological Sciences, Royal Holloway University of London, Egham TW20 0EX, UK. ⁴Institució Catalana de Recerca i Estudis Avançats (ICREA), Ps. Lluís Companys 10, 08010 Barcelona, Spain.

*Present address: Institute of Science and Technology Austria, 3400 Klosterneuburg, Austria. †Present address: Department of Comparative Development and Genetics, Max Planck Institute for Plant Breeding Research, 50829 Cologne, Germany. ‡Present address: INRA, Joint Research Unit 'Biology and Genetics of Plant-Pathogen Interactions', Campus International de Baillarguet, 34398 Montpellier Cedex 5, France. ¶Present address: Institute of Botany, Chinese Academy of Sciences, Kunming 650201, China.

**These authors contributed equally to this work

‡† Author for correspondence (jaume.martinez@cragenomica.es)

trafficking between the cytoplasm and the nucleus. Despite structural differences, there are conserved functional similarities between NPCs from plants and other organisms (Raices and D'Angelo, 2012; Parry, 2013; Tamura and Hara-Nishimura, 2013). The NPC consists of multiple copies of at least 30 different nucleoporins (NUPs), which together form a channel-like structure of octagonal symmetry organized in three elements: a nuclear basket, a central pore, and cytoplasmic fibrils. Depending on their position within the NPC, NUPs can be classified into two major categories: scaffold (which form the rigid skeleton) and peripheral (which form a selective barrier for the diffusion of molecules larger than ~60 kDa). Proteomic approaches have identified several *Arabidopsis* NUPs belonging to both categories (Tamura et al., 2011). Functionally, *Arabidopsis* NUP-deficient single-mutant lines display several pleiotropic developmental alterations, such as early flowering, disrupted circadian function and even embryo lethality (MacGregor et al., 2013; Parry, 2014). However, whether the NPC and/or individual NUPs impact photomorphogenic responses and/or light signaling remains virtually unexplored.

To identify new regulatory components of the SAS, a high-throughput genetic screen was performed after EMS mutagenesis of a shade-responsive luciferase reporter line, PHYB:LUC (hereafter PBL), which expresses the *Luciferase* (*LUC*) gene under the control of the *Arabidopsis* *PHYB* promoter in the Ws-2 genetic background (Kozma Bognar et al., 1999). As a result we identified *dracula* (*dra*) mutants, which exhibit an attenuated luciferase response to low R:FR light. One of the mutants identified was *dracula1* (*dra1*), which carries the novel *phyA*^{G773E} mutation (Wang et al., 2011). Here, we present *dra2*, which affects a gene encoding NUP98A, a component of the NPC in plants (Xu and Meier, 2008; Tamura et al., 2011). Our results suggest that an intact NPC is essential for proper SAS responses. Furthermore, our comparative analyses of several NUP-deficient mutant seedlings indicate that *DRA2* also has a specific role in the early shade regulation of *PAR* gene expression.

RESULTS AND DISCUSSION

The *dra2-1* mutation alters the SAS seedling response

After EMS mutagenesis of the PBL reporter line, we performed a large-scale screen looking for mutant seedlings exhibiting significantly altered luciferase activity after 2 h of simulated shade ($P < 0.001$) (Wang et al., 2011). One of the mutants isolated, *dra2-1*, showed an attenuated luciferase activity after just 1 h of white light plus far-red light (W+FR) treatment (Fig. 1A). Additional molecular analyses (see below) indicated that *LUC* expression in response to shade was attenuated in *dra2-1*. Adult *dra2-1* plants grown under standard greenhouse (long-day) conditions displayed a range of morphological phenotypes, such as small rosettes, short flowering stems and siliques, and a general weak aspect; moreover, these plants were early flowering under both long- and short-day conditions (Fig. S1A–C). Mutant seedlings grown under continuous white light (W) had long hypocotyls and strongly hyponastic cotyledons (Fig. 1B). More importantly, the seedling response to W+FR in terms of hypocotyl, cotyledon and primary leaf elongation was attenuated in *dra2-1* compared with PBL (Fig. 1C, Fig. S1D).

DRA2 encodes *Arabidopsis* NUP98A

Genetic analyses indicated that the mode of inheritance of the *dra2-1* line is monogenic and recessive. After positional cloning, a candidate interval of 270 kb at the upper arm of chromosome 1, flanked by the *nga63* (between genes *At1g09910* and *At1g09920*) and *cer458005* (*At1g10560*–*At1g10570*) markers, was defined (Fig. S2A). While this work was in progress we learned that

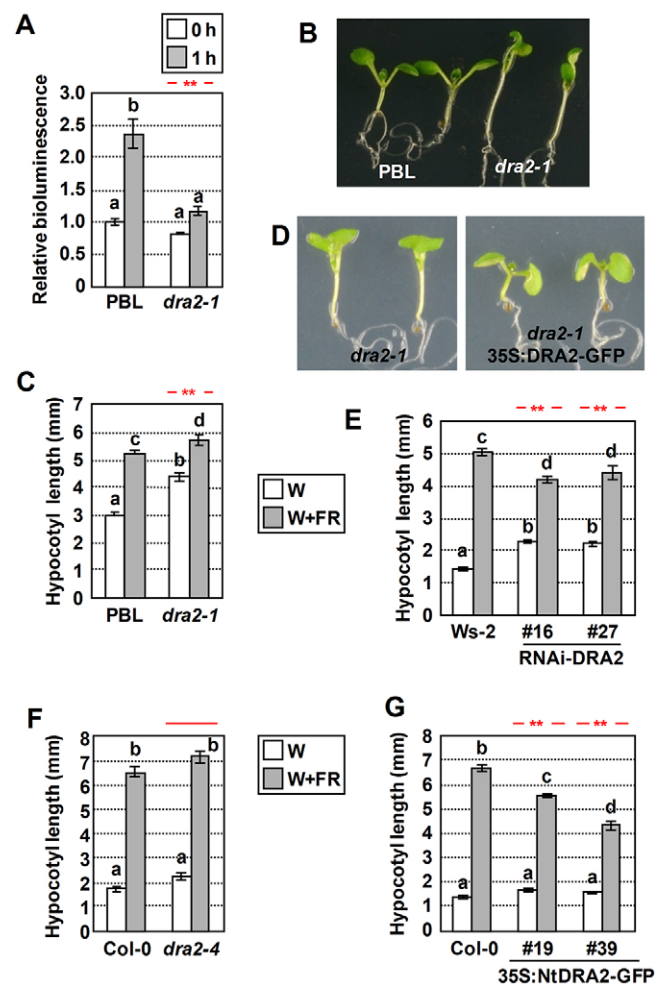


Fig. 1. *Arabidopsis dra2-1* seedlings show a reduced response to simulated shade. (A) Seven-day-old white light (W)-grown seedlings of PBL and *dra2-1* (0 h) were transferred to white plus far-red light (W+FR) for 1 h. Data represent mean \pm s.e. bioluminescence measurements from at least 20 seedlings relative to the activity levels in PBL seedlings at 0 h. (B) Representative 7-day-old PBL and *dra2-1* seedlings grown under W. (C) Length of hypocotyls of PBL and *dra2-1* in response to W+FR. Seeds were germinated and grown for 2 days under W and then either kept under W or transferred to W+FR for 5 more days. (D) Representative 7-day-old seedlings of *dra2-1* and *dra2-1*;35S:DRA2-GFP. (E) Hypocotyl length of wild-type (Ws-2) and transgenic 35S:RNAi-DRA2 seedlings in response to simulated shade. (F,G) Hypocotyl length of wild-type (Col-0) and mutant *dra2-4* seedlings (F) and of transgenic 35S:NtDRA2-GFP seedlings (G) in response to simulated shade. (A,C,E–G) Different lowercase letters denote significant differences (one-way ANOVA with Tukey test, $P < 0.05$) among means; and red asterisks indicate significant differences (two-way ANOVA, $**P < 0.01$) between the mutant and wild-type genotypes in response to W+FR. Red bars without an asterisk indicate the absence of any statistically significant difference from the response of wild-type seedlings to simulated shade.

mutant alleles of *Arabidopsis* genes encoding NUPs display long hypocotyls and/or early-flowering phenotypes (Ferrandez-Ayala et al., 2013; Parry, 2013; Tamura and Hara-Nishimura, 2013). *At1g10390*, a gene within the candidate interval annotated to encode an NUP, was sequenced in *dra2-1* and PBL. In *dra2-1* plants, *At1g10390* carries a G-to-A transition, which would result in a nonsense mutation at Trp780 of the protein (Fig. S1E). Hereafter, and based on results shown below, we will refer to this gene as *DRACULA2* (*DRA2*). First, co-segregation analyses of the mutant phenotype and the identified mutation indicated that the only allele

detected among the phenotypically mutant seedlings was *dra2-1*, a result consistent with the recessive nature of this mutant (Fig. S1F). Second, the recessive *dra2-1* mutation was complemented with a constitutively expressed translational fusion of *DRA2* to the *Green fluorescent protein (GFP)* marker gene (35S:*DRA2*-GFP lines) at both the seedling and adult stages (Fig. 1D, Fig. S2B–D). Third, transgenic seedlings overexpressing an RNAi directed towards *DRA2* (35S:RNAi-*DRA2* lines, generated in the Ws-2 background) showed a similar phenotype to *dra2-1* seedlings. This RNAi was directed towards a region that diverged between *DRA2* and its closest homolog in the *Arabidopsis* genome (*At1g59660*), which we named *DRA2-LIKE (DRAL)* (Fig. S3A). The strong hyponastic cotyledons characteristic of *dra2-1* seedlings were only observed in a few 35S:RNAi-*DRA2* lines that either had severe growth problems and died before producing seeds or lost their characteristic phenotype in the following generation (Fig. S3B). Nonetheless, transgenic seedlings with a mild phenotype had longer hypocotyls than Ws-2 under W; importantly, in these lines the hypocotyl response to W+FR was attenuated compared with Ws-2 (Fig. 1E, Fig. S3C). Together, these results indicated that *At1g10390* is the causal gene for the phenotype of *dra2-1*.

Lines carrying T-DNA insertions disrupting *At1g10390* were identified in the Col-0 background. We named these mutants *dra2-2* to *dra2-5*. In these lines, except *dra2-2*, T-DNA insertions mapped within the main ORF and are likely to perturb *DRA2* function (Fig. S4A). At least one of these alleles is null, as indicated by the absence of detectable *DRA2* mRNA in *dra2-4* seedlings (Fig. S4B). Nonetheless, all analyzed *dra2* mutant seedlings had longer hypocotyls than Col-0 under W. However, they did show an almost wild-type response to simulated shade, in contrast to *dra2-1* seedlings (Fig. 1F, Fig. S4C). Overall, these T-DNA mutants identified in Col-0 displayed a mild or weak phenotype, a result consistent with published information about an additional knockout allele of *DRA2* (Parry, 2014). The strong phenotype shown by the *dra2-1* mutant, particularly its hyponastic cotyledons, was severely reduced after four *dra2-1*×Col-0 backcrosses (Fig. S4D). These results suggested that the genomic Col-0 background (very likely near the *DRA2* locus) strongly modifies the mutant phenotype caused by *DRA2* loss of function.

DRA2 encodes an NUP of 1041 amino acids, with a molecular mass of ~105 kDa, and that contains phenylalanine-glycine (FG) repeats (Xu and Meier, 2008; Tamura and Hara-Nishimura, 2013). A number of yeast and vertebrate NUPs have FG repeats, which are thought to provide transient, low-affinity binding sites for transport receptors. Two genes encoding an NUP-like FG repeat-containing protein can be identified by sequence similarity searches with mammalian Nup98 (mNup98) in the *Arabidopsis* database: *DRA2* (*At1g10390*, *NUP98A*) and *DRAL* (*At1g59660*, *NUP98B*) (Xu and Meier, 2008). Proteomic analyses of the NPC identified several *Arabidopsis* NUPs, including *DRA2* and *DRAL* (Tamura et al., 2011). The N-terminal region of mNup98 (NtNup98) contains 39 FG repeats (Table S1) (Radu et al., 1995; Griffiths et al., 2002). The C-terminal region of mNup98 (CtNup98) mediates its interaction with the NPC (Hodel et al., 2002) and contains a minimal cleavage domain that is evolutionarily conserved also in the C-terminal part of *Arabidopsis* *DRA2* and *DRAL*, which suggests that the C-terminal region of *DRA2* mediates the interaction with the NPC in plants. Overexpression of mammalian NtNup98 fused to GFP results in a dominant-negative form that interferes with endogenous mNup98 activity (Liang et al., 2013). Overexpression of the N-terminal part of *DRA2* (amino acids 1–779, NtDRA2) fused to *GFP* in Col-0 (35S:NtDRA2-GFP lines) caused stunted growth. More importantly, transgenic seedlings had slightly

longer hypocotyls than Col-0 under W and displayed an attenuated response to simulated shade (Fig. 1G), a phenotype resembling that of the strong *dra2-1* and 35S:RNAi-*DRA2* seedlings. The NtDRA2 fragment contains all the FG repeats and seems unable to bind to the NPC (Table S1), suggesting that NtDRA2 might also behave as a dominant-negative form towards *DRA2* in the Col-0 background. Interference by NtDRA2 with the function of *DRAL* might further explain the more severe phenotype of these transgenic lines compared with the single null *dra2* mutants in the Col-0 background.

Loss of function of different NUPs causes an altered hypocotyl response to simulated shade

To evaluate whether the sole disruption of NPC function results in an altered SAS phenotype, we tested mutants affected in several other NUPs, such as SUPPRESSOR OF AUXIN RESISTANCE 1 (SAR1; also known as NUP160), SAR3 (also known as NUP96) (Parry et al., 2006), TRANSCURVATA1 (TCU1; also known as NUP58) (Ferrandez-Ayela et al., 2013), NUP54 and NUP62 (Fig. S5). Structurally, these *Arabidopsis* NUPs contain different domains: SAR1 and SAR3 contain an α -solenoid domain; SAR1 also contains a β -propeller; NUP54, TCU1, NUP62 and *DRA2* contain FG repeats; and NUP54, TCU1 and NUP62 also contain a coiled-coil region (Tamura and Hara-Nishimura, 2013). Functionally, these NUPs represent different types of components of the NPC: SAR1 and SAR3 are predicted to be scaffold NUPs; and NUP54, TCU1 and NUP62, together with *DRA2*, are considered to be peripheral NUPs attached to the membrane-embedded scaffold (D'Angelo et al., 2009; Tamura and Hara-Nishimura, 2013).

After analyzing the hypocotyl response to W and W+FR, mutant alleles were classified as displaying mild (*sar3-3*, *nup54-1*, *nup54-*

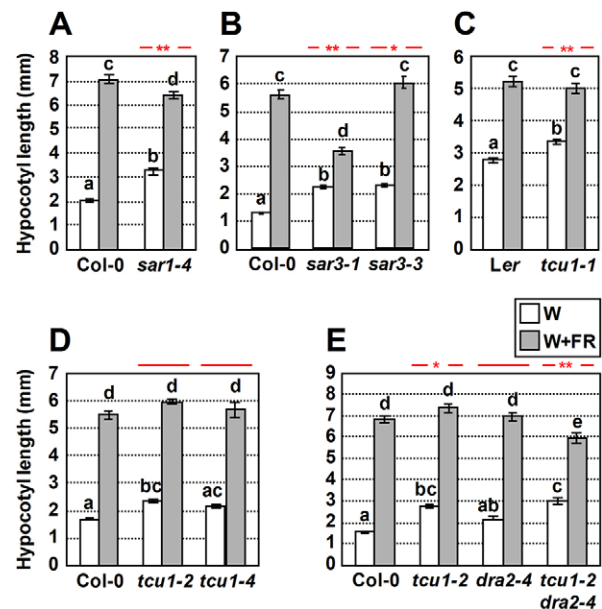


Fig. 2. Seedlings deficient in several NUPs show an altered response to simulated shade. (A–D) Hypocotyl length of wild-type (Col-0 and Ler) and (A) *sar1-4*, (B) *sar3-1* and *sar3-3*, (C) *tcu1-1*, (D) *tcu1-2* and *tcu1-4* mutant seedlings in response to simulated shade. (E) Genetic analysis of functional redundancy between *TCU1* and *DRA2* in the Col-0 ecotype. Hypocotyl length of wild type, *tcu1-2*, *dra2-4* and *tcu1-2; dra2-4* mutants in response to simulated shade. Seedlings were grown as indicated in Fig. 1C. Different lowercase letters denote significant differences (one-way ANOVA with Tukey test, $P < 0.05$) among means; red asterisks indicate significant differences (two-way ANOVA, $*P < 0.05$, $**P < 0.01$) between the mutant and wild-type genotypes in response to W+FR.

2, *tcu1-2* and *tcu1-4*) or strong (*sar1-4*, *sar3-1*, *nup62-1*, *nup62-2* and *tcu1-1*) phenotypes compared with the response of the corresponding wild-type seedlings (Fig. 2A–D, Fig. S5). The mild alleles mimicked the response of mutants *dra2-2* to *dra2-5* (in the Col-0 background), whereas the strong alleles responded similarly to *dra2-1* (an allele in the Ws-2 background). The phenotypic strength of loss-of-function *tcu1* alleles was likewise affected by the genetic background: *tcu1-2* and *tcu1-4* (in Col-0) were mild, whereas *tcu1-1* (in Ler) was strong (Fig. 1, Fig. S4). We hypothesized that the genetic background influence could reflect different levels of impairment of NPC activity, probably caused by variations in basal NUP activity among the accessions compared. Indeed, an increase in phenotype severity has been observed by other authors in double NUP mutants (Ferrandez-Ayela et al., 2013; Parry, 2014), suggesting a relationship between the strength of the phenotypes analyzed and the level of impairment of NPC function. Consistently, double mutants involving weak alleles of *DRA2* (e.g. *dra2-3*, *dra2-4* and *dra2-5*) and *TCU1* (*tcu1-2*) showed a shade-induced hypocotyl response similar to that of single mutants carrying strong alleles (Fig. 2E, Fig. S5F).

DRA2 participates in mRNA export from the nucleus

SAR1 and SAR3 were reported to participate in mRNA export from the nucleoplasm to the cytoplasm (Dong et al., 2006; Parry et al., 2006). To address whether *DRA2* also participates in this transport-related activity of the NPC, *in situ* hybridization to localize poly(A)⁺

mRNA was carried out in 7-day-old wild-type and NUP mutant seedlings. Using an oligo(dT)₅₀ probe end-labeled with fluorescein, nuclear retention of poly(A)⁺ RNA was clearly discernible in seedlings of the strong alleles *sar3-1* and *dra2-1*, but not in the corresponding wild type and the weak *dra2-3* and *dra2-4* mutants (Fig. 3A). These results suggest that *DRA2* is required for mRNA nucleocytoplasmic trafficking in a genetic background-dependent manner and support the proposal that *dra2-1* seedlings have an impaired NPC.

Expression of *DRAL*, the closest paralog of *DRA2*, was strongly upregulated (18-fold) in *dra2-1* seedlings (Fig. 3B), but only moderately increased (3-fold) in weak *dra2-4* mutant seedlings (Fig. S6). *DRAL* expression was also upregulated in single or double NUP-deficient mutants with strong phenotypes, such as *sar1-4* (10-fold), *sar3-1* (14-fold), *tcu1-1* (7-fold) and *dra2-4;tcu1-2* (11-fold), and to a lesser extent in the weak *tcu1-2* (2- to 3-fold) and *sar3-3* (3-fold) mutants (Fig. 3B, Fig. S6). *DRAL* expression was also strongly upregulated in RNAi-*DRA2* seedlings with downregulated *DRA2* expression (Fig. 3C). A significant increase in the expression of *DRAL* and other genes involved in nuclear transport, such as *RNA EXPORT FACTOR 1* (*RAE1*) and *NUCLEAR EXPORTIN 1B* (*XPO1B*), was recently reported in seedlings of three different NUP-deficient mutants: *nup62-2*, *nup160-1* (a mutant allele of *SAR1* not analyzed in our work) (Parry, 2014) and *high expression of osmotically responsive genes 1* (*hos1*) (MacGregor et al., 2013). These results revealed a possible feedback relationship between

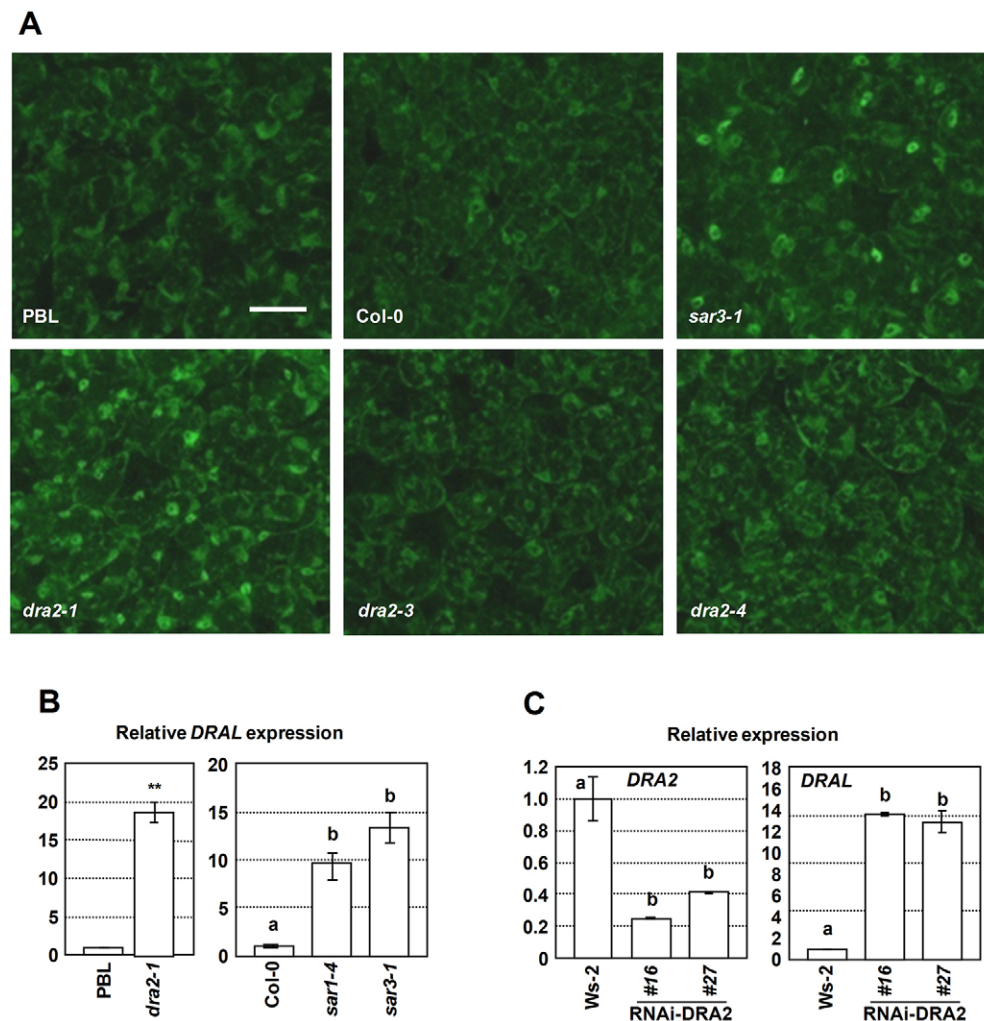


Fig. 3. Several NUP-deficient mutants display similar defects in the export of mRNA and changes in *DRAL* gene expression. (A) *In situ* hybridization of poly(A)⁺ RNA was performed in cotyledons of 7-day-old seedlings grown under W. Seedlings from wild type (Col-0, Ws-2) and *dra2-1*, *sar3-1*, *dra2-3* and *dra2-4* mutants were analyzed with fluorescein-tagged oligo(dT) probe. Fluorescence was visualized by confocal microscopy. Scale bar: 40 μ m. (B) *DRAL* gene expression analysis in seedlings of wild type (PBL or Col-0), *dra2-1*, *sar1-4* and *sar3-1* mutants. Seedlings were grown under continuous W for 7 days. (C) *DRA2* and *DRAL* gene expression analysis in seedlings of wild type (Ws-2) and the two RNAi-*DRA2* independent transgenic lines shown in Fig. 1E. Transcript abundance of *DRAL* and *DRA2* (both normalized to *UBQ10*) is shown. Seedlings were grown under continuous W for 7 days. (B,C) Values are the mean \pm s.e. of three to six independent biological replicates relative to wild-type values. Asterisks indicate significant differences (Student's *t*-test, ***P* < 0.01) relative to wild-type seedlings; the different lowercase letters denote significant differences (one-way ANOVA with Tukey test, *P* < 0.05) among means.

impaired NPC function and the expression of genes involved in nuclear transport (Parry, 2014). Although it is unclear if this feedback regulation has any biological relevance (e.g. if it results in a compensatory mechanism to increase the rate of nuclear transport), our observations do indicate a positive correlation between *DRAL* expression levels and the strength of the physiological SAS phenotype. Since the strong mutants analyzed display a clear poly(A)⁺ RNA nuclear retention that reflects defects in the NPC (Fig. 3A) (Dong et al., 2006; Parry et al., 2006), our results support the proposal that *DRAL* upregulation is a reliable marker for NPC dysfunction.

***dra2-1* seedlings display an attenuated early induction of *PAR* gene expression**

We reasoned that other shade-regulated responses, such as the induction of *PAR* gene expression, might also be altered in NUP-deficient mutants. We therefore analyzed the accumulation of transcripts of shade-responsive genes in *dra2-1* and PBL seedlings before and after W+FR exposure (0, 1, 2 and 4 h). As expected, the transgenic marker *LUC* and endogenous *PHYB*, *PIL1* and *HFR1* were rapidly induced after W+FR treatment. However, their shade-induced expression was significantly attenuated in *dra2-1* compared with PBL control seedlings (Fig. 4A), indicating that *DRA2* promotes the shade-induced expression of these genes. *ATHB2*, another well-known shade-induced gene, was unaffected by simulated shade in *dra2-1* seedlings (Fig. S7). In *sar1-4* and *sar3-1* seedlings, *PHYB* shade-induced expression was also attenuated compared with the Col-0 control, whereas that of *PIL1* and *HFR1* was enhanced (rather than reduced) (Fig. 4B, Table S2). Therefore, we deduced that *SAR1* and *SAR3* participate, like *DRA2*, in promoting the shade-triggered activation of *PHYB* expression, but differ from *DRA2* in their specific effect of *PIL1* and *HFR1* gene expression. No significant differences in the early shade-induced expression of these genes were found between wild-type (*Ler*) and strong *tcu1-1* mutant seedlings (Fig. 4C). These observations indicate that rapid and efficient shade-induced gene expression requires specific NUPs, such as *DRA2*, *SAR1* and *SAR3*, and that these NUPs appear to have different roles in this process.

Several of the *Arabidopsis* NUP-deficient single mutant lines are early flowering, including the strong *sar1*, *sar3* (Dong et al., 2006; Parry et al., 2006), *tcu1* (Ferrandez-Ayala et al., 2013), *nuclear pore anchor* (*nua*; also known as *tpr*) (Jacob et al., 2007; Xu et al., 2007), *nup136* (Tamura et al., 2011), *nup62* (Zhao and Meier, 2011), *hos1* (MacGregor et al., 2013) and *dra2* mutants (Fig. S1). More recently, analyses of NUP-deficient mutants, such as *hos1*, *sar1*, *nua* and *nup107*, also showed disrupted circadian function and cold-regulated gene expression, suggesting that these additional phenotypes are also a general consequence of disrupting NPC function in plants (MacGregor et al., 2013). Our analyses indicated that some of these mutants share additional phenotypes, such as upregulation of *DRAL* expression, long hypocotyls under W and/or attenuated hypocotyl elongation in response to simulated shade (Figs 1–3, Figs S5, S6). The shared pleiotropic phenotypes of different NUP-deficient mutants is likely to be a downstream consequence of a generic disruption of the NPC and the associated effect on its main function, that of nucleocytoplasmic trafficking. These phenotypes can therefore be referred to as transport dependent (Capelson and Hetzer, 2009; Raices and D'Angelo, 2012).

By contrast, attenuation of early shade-triggered gene expression is not a general phenomenon caused by nonspecific depletion of any

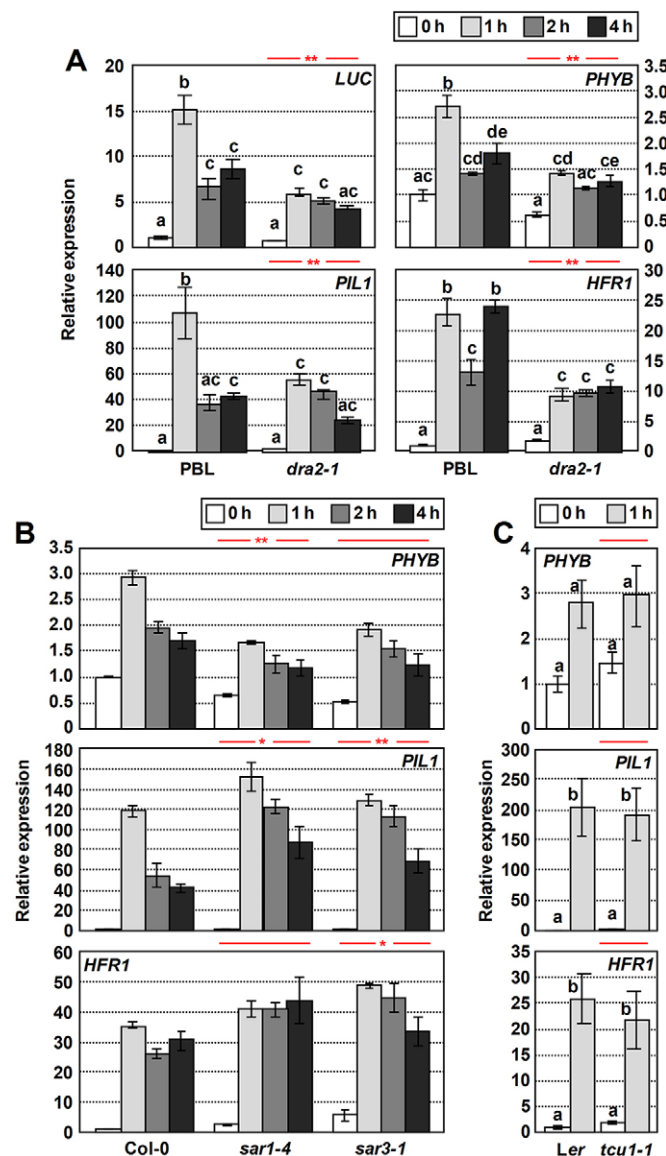


Fig. 4. Shade-induced expression is attenuated in *dra2-1* but not in other NUP mutants. (A,B) Expression analysis of *PAR* genes in seedlings of wild-type (PBL or Col-0) and (A) *dra2-1*, (B) *sar1-4* or *sar3-1* seedlings treated for 0, 1, 2 and 4 h with W+FR. (C) Expression analysis of *PAR* genes in wild-type (*Ler*) and *tcu1-1* seedlings treated for 0 and 1 h with W+FR. Seedlings were grown under continuous W for 7 days. Transcript abundance is shown for the indicated genes, normalized to *UBQ10*. Values are the mean \pm s.e. of three independent qPCR biological replicates relative to wild-type values at 0 h. (A,C) Different lowercase letters denote significant differences (one-way ANOVA with Tukey test, $P < 0.05$) among means. (B) The results of the one-way ANOVA with Tukey test ($P < 0.05$) are presented in Table S2. Red asterisks indicate significant differences (two-way ANOVA, $*P < 0.05$, $**P < 0.01$) between the mutant and wild-type genotypes in response to W+FR.

NPC component. Indeed, whereas loss of *TCU1* had no impact at all on *PAR* gene expression in response to low R:FR, other NUPs (*SAR1*, *SAR3* and *DRA2*) modulated the shade-induced expression of specific genes in similar or even opposing directions, as observed in *dra2-1*, *sar1-4* and *sar3-1* seedlings (Fig. 4). These results support the proposal that a number of different plant NUPs have specific roles in the control of gene expression besides their transport-dependent functions as components of the NPC. Indeed, an increasing body of evidence (largely from studies in yeast and mammals) suggests that some NUPs are also involved in regulating

gene expression, a role that has been referred to as transport independent (Capelson and Hetzer, 2009; Raices and D'Angelo, 2012). In particular, animal Nup98 appears to regulate gene expression by binding directly to chromatin and/or by stabilizing some mRNAs in cell cultures (Capelson et al., 2010; Kalverda et al., 2010; Singer et al., 2012). This is proposed to occur because mNup98 is dynamic, i.e. it is associated with the NPC and shuttles between the nucleus and the cytoplasm (Griffis et al., 2002). In plants, only NUP136 was shown to be dynamic, although this feature was not related with any transport-independent activity, such as the regulation of specific genes (Tamura et al., 2011).

DRA2 is a dynamic NUP

A translational fusion between GFP and mNup98 was reported to move between the nucleoplasm and the NPC, as well as between the nucleus and the cytoplasm, indicating that this is a dynamic NUP (Powers et al., 1997; Fontoura et al., 2000; Griffis et al., 2002). This dynamism appears to be related to the role of mNup98 in gene regulation (i.e. it is transport independent), since the mobility of mNup98 within the nucleus and at the NPC is dependent on ongoing transcription by RNA polymerases (Griffis et al., 2002; Raices and D'Angelo, 2012). mNup98 localized in the nucleoplasm and the cytoplasm can associate with some spots (mostly nuclear) of unknown identity. The GFP fusion of the animal N-terminal Nup98 (NtNup98-GFP) is also localized preferentially in spots within the nucleus (Griffis et al., 2002; Kalverda et al., 2010). Similarly, transient overexpression of NtDRA2-GFP in leek epidermal cells resulted in GFP activity in both cytoplasmic and nuclear spots (Fig. 5A). *Arabidopsis* 35S:NtDRA2-GFP seedlings also displayed fluorescence in cytoplasmic and nuclear-localized spots (Fig. 5B).

In 35S:NtDRA2-GFP seedlings, *DRAL* expression was also significantly upregulated (8-fold), indicating that overexpression of NtDRA2 interferes with the transport-dependent activity of the NPC. More importantly, shade-induced *HFR1* and *PIL1* expression was also significantly attenuated (Fig. 5C), suggesting that this truncated form also interferes with transport-independent activities of DRA2. These results support our hypothesis that the FG-containing NtDRA2 fragment has a dominant-negative effect on the expression of DRA2-regulated genes, an activity also observed for the N-terminal mNup98 fragment (Liang et al., 2013). Since NtDRA2 does not localize in the NPC, it should interfere with pools of DRA2 that localize either in the nucleus or the cytoplasm.

To verify DRA2 subcellular localization, we aimed to use our 35S:DRA2-GFP lines. Although high levels of *DRA2* expression were detected in these lines (Fig. S8A) and the DRA2-GFP fusion was active to complement the *dra2-1* mutation (Fig. 1D), no GFP fluorescence was detected in these seedlings. Leaves of *Nicotiana benthamiana* agroinfiltrated to transiently overexpress *DRA2-GFP* also lacked any detectable GFP fluorescence (Fig. 6A). The C-terminal end of DRA2 contains a conserved peptide motif that is necessary for the autoproteolytic cleavage of vertebrate Nup98 (Parry et al., 2006). Because this sequence might contribute to the lack of fluorescence activity of DRA2-GFP, we generated a new version of the protein with GFP tags at both the C-terminal and N-terminal ends (35S:GFP-DRA2-GFP). Transient overexpression of this fusion in agroinfiltrated leaves of *N. benthamiana* showed green fluorescence in cytoplasm and nucleoplasm spots (Fig. 6B, upper panels, Fig. S8B). The analysis of confocal series of optical sections further showed that, unlike NtDRA2-GFP, the GFP-DRA2-GFP fluorescence was detected in both the nuclear rim and inside the nucleus but excluded from the nucleolus (Fig. 6B, lower panels, Fig. S8C). This subcellular localization is consistent with DRA2

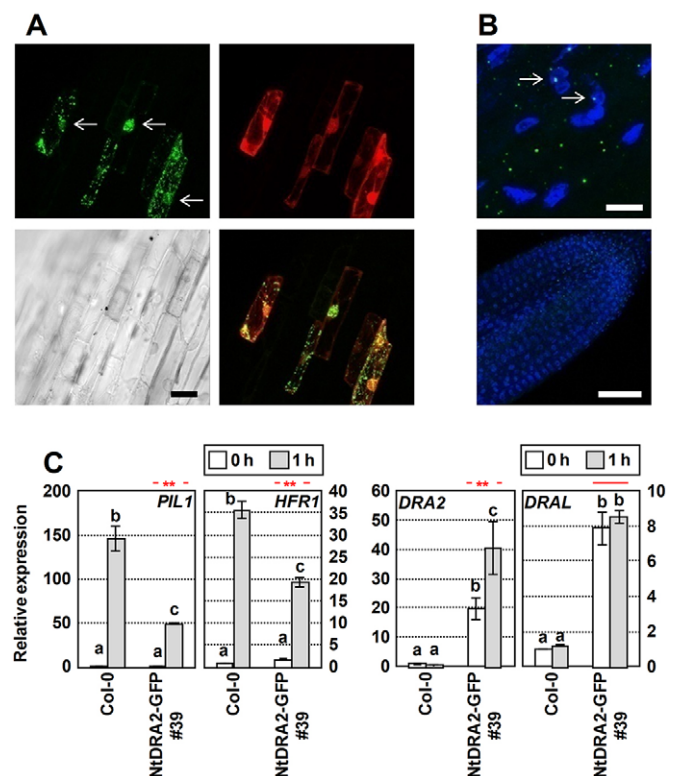


Fig. 5. NtDRA2 acts as a dominant-negative form. (A,B) Subcellular location of the NtDRA2-GFP fusion protein in (A) leek onion epidermal cells and (B) roots of transgenic *Arabidopsis* seedlings. (A) Leek cells were co-bombarded with constructs encoding NtDRA2-GFP (green, top left) and DsRED (red, top right). Fluorescence was analyzed after 24 h. Overlay fluorescence (bottom right) and bright-field (bottom left) images are shown. (B) Roots correspond to 35S:NtDRA2-GFP seedlings grown under continuous W for 7 days; root cells were stained using DAPI to identify nuclei (blue). Arrows (A,B) point to the GFP activity located in nuclei. (C) Expression analysis of *PIL1*, *HFR1*, *DRA2* and *DRAL* in wild-type and 35S:NtDRA2-GFP seedlings treated for 0 and 1 h with W+FR. Seedlings were grown under continuous W for 7 days. Transcript abundances were analyzed as indicated in Fig. 4. Different lowercase letters denote significant differences (one-way ANOVA with Tukey test, $P < 0.05$) among means; red asterisks indicate significant differences (two-way ANOVA, $**P < 0.01$) between the transgenic and wild-type genotypes in response to W+FR. Scale bars: 50 μ m, except 10 μ m in lower image in B.

being part of the NPC and also fits with the idea that DRA2, like mNup98, is a dynamic NUP rather than just a key structural element of the NPC.

In summary, based on (1) the functionality and subcellular localization of the dominant-negative NtDRA2-GFP protein, and (2) the subcellular localization of full-length GFP-DRA2-GFP, we concluded that, like its mammalian counterpart Nup98, DRA2 is a dynamic NUP.

Beyond nucleocytoplasmic transport: a dual role for dynamic DRA2 in SAS regulation?

Our work highlights the importance of nucleocytoplasmic transport for the adaptation of plants to changing light environments (Fig. 7). After phytochrome inactivation induced by perception of low R:FR light, increased dephosphorylation of PIF proteins, which is likely to cause enhanced DNA binding to their target genes (Li et al., 2012), results in the rapid induction of *PAR* gene expression, some of which encode transcriptional regulators that are instrumental for SAS responses. These changes directly or indirectly affect the endogenous hormonal pathways by altering the levels of, or

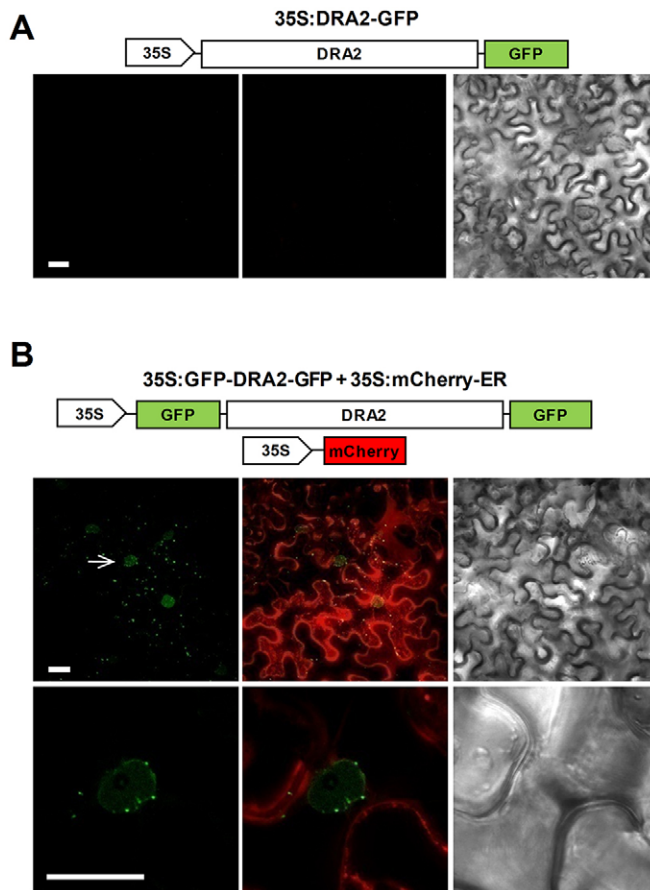


Fig. 6. DRA2 is localized in the cytoplasm, the nucleoplasm and the nuclear rim. (A) Confocal images of leaf tobacco cells agroinfiltrated with construct DRA2-GFP. The construct used is illustrated above. (B) Confocal images of leaf tobacco cells co-agroinfiltrated with constructs GFP-DRA2-GFP and mCherry-ER. The constructs used are illustrated above. The top row shows a z-stack of ten optical sections; the arrow points to the nucleus magnified in the bottom row of images, which correspond to a single and intermediate optical section (see Fig. S8). (A,B) In each series of three images, green fluorescence (left), red and green fluorescence overlay (center) and bright-field (right) are shown. In each series, images are at the same scale. Scale bars: 20 μ m.

sensitivity to, hormones, such as auxins, brassinosteroids and gibberellins (Li et al., 2012; Bou-Torrent et al., 2014). The NPC components SAR1 and SAR3 have been shown to play a role in

auxin signaling and development (Parry et al., 2006). Although it is currently unknown whether DRA2 and other NUPs also play a role in auxin signaling, it is possible that the attenuated hypocotyl elongation in response to simulated shade shared by different NUP-defective mutants (Figs 1, 2, Fig. S5) might be related to general alterations in hormone-regulated development caused by a transport-dependent activity of the NPC (Fig. 7). Further studies are needed to explore this possibility.

Besides a role as part of the NPC, DRA2 has an additional and unique function as a regulator of genes actively transcribed immediately after shade stimulus perception. How can DRA2 affect shade-induced gene expression? We envisage two alternative mechanisms. First, its dynamic nature might provide DRA2 with the ability to specifically alter the nucleocytoplasmic movement of light-signaling components, such as phytochromes, which are known to partition between the cytoplasm and nucleus in a light-dependent manner. A defect in phytochrome partitioning would be expected to result in a global impairment of shade-regulated activities, such as the early induction of gene expression. However, shade-induced *HFR1*, *PHYB* and *PIL1* expression was impaired in *dra2-1* seedlings (Fig. 4), whereas *ATHB2* expression was unaffected (Fig. S7), despite the fact that shade-induced expression of *ATHB2*, *PIL1* and other *PAR* genes has been shown to be affected by altered levels of phyA or phyB (Devlin et al., 2003; Roig-Villanova et al., 2006). We therefore believe that this first scenario is unlikely. A second possibility is the control of gene expression by direct binding to chromatin, as proposed for metazoan Nup98 (Light et al., 2013). This would represent a transport-independent mechanism in which DRA2 accesses chromatin regions corresponding to shade-induced genes (Fig. 7). Work is in progress to explore this second possibility with a view to identifying the precise molecular mechanisms by which DRA2 selectively influences the transcription of early shade-regulated genes.

MATERIALS AND METHODS

Plant material and growth conditions

Arabidopsis plants for seed production and for crosses were grown in the greenhouse as described (Martínez-García et al., 2002). All experiments were performed with surface-sterilized seeds sown on Petri dishes with solid growth medium without sucrose [GM–: 0.215% (w/v) MS salts plus vitamins, 0.025% (w/v) MES pH 5.8] (Roig-Villanova et al., 2006), unless otherwise stated. After stratification (3–5 days) plates were incubated in an I-36VL growth chamber (Percival Scientific) at 22°C under W provided by four cool-white vertical fluorescent tubes (25 μ mol m^{–2} s^{–1} of photosynthetically active radiation; R:FR of 3.2–4.5). Simulated shade (W+FR) was generated by enriching W with supplementary FR provided by QB1310CS-670-735 LED

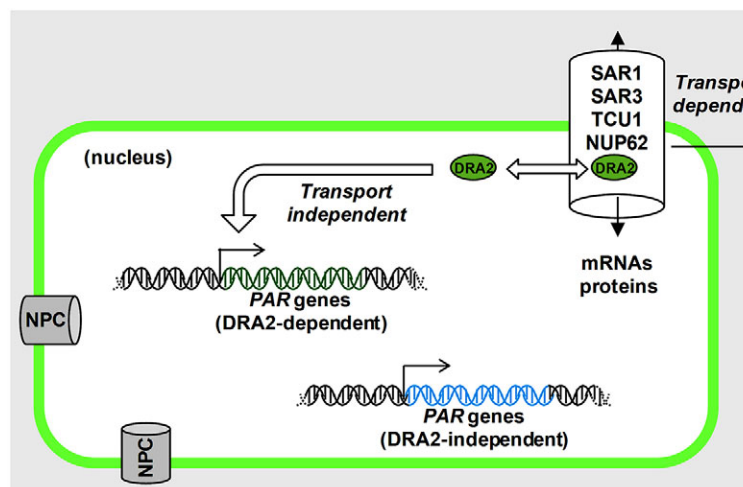


Fig. 7. The dual role of DRA2 in regulating different aspects of the SAS in seedlings. The model shows a transport-dependent function in the regulation of SAS hypocotyl elongation, which is shared with several other NPC components (such as SAR1, SAR3, TCU1 and NUP62, as analyzed in this work), and a transport-independent function in the regulation of shade-induced gene expression, which is postulated to be unique to DRA2. The latter function is likely to be related to the dynamics of DRA2, which can shuttle between the NPC located in the nuclear envelope, and the nucleus and cytoplasm.

hybrid lamps (Quantum Devices; $25 \mu\text{mol m}^{-2} \text{s}^{-1}$ of photosynthetically active radiation; R:FR ratio of 0.05). Fluence rates were measured using an EPP2000 spectrometer (StellarNet) or a Spectrosense2 meter associated with a four-channel sensor (Skye Instruments) (Martínez-García et al., 2014). For gene expression analyses, seeds were sown on filter paper or a nylon mesh on top of GM-. For luciferase imaging, GM- medium was supplemented with 2% (w/v) sucrose.

The mutants used in this work, accession numbers of the mutated genes, the molecular nature of their mutations, their genetic backgrounds and the sequences of the oligonucleotides used for their genotyping by PCR are provided in the supplementary Materials and Methods.

Seedling morphometry

Hypocotyl, cotyledon and primary leaf lengths were measured as described (Roig-Villanova et al., 2007; Sorin et al., 2009) and see the supplementary Materials and Methods. At least 15 seedlings were used for each treatment. Experiments were repeated three to five times and a representative experiment is shown. Statistical analyses of the data by one-way ANOVA with Tukey HSD post-hoc comparison, and two-way ANOVA, were performed using GraphPad Prism (version 4.00 for Windows).

Construction of transgenic lines

Transgenic 35S:DRA2-GFP and 35S:RNAi-DRA2 lines were in the Ws-2 background. Transgenic 35S:NtDRA2-GFP lines were in the Col-0 background. Details of their generation are given in the supplementary Materials and Methods.

Gene expression analysis

Total RNA was isolated from seedlings using the RNeasy Plant Mini Kit (Qiagen) or the Maxwell 16 LEV simplyRNA Tissue Kit (Promega). Reverse transcriptase and quantitative PCR (qPCR) analyses of gene expression were performed as described (Sorin et al., 2009). The *UBQ10* gene was used as a control for normalizations. Three biological replicates for each sample were assayed. Further details, including primer sequences, can be found in the supplementary Materials and Methods. Statistical analyses of the data were performed as described above.

Whole-mount *in situ* hybridization of poly(A)⁺ RNA

Poly(A)⁺ RNA *in situ* hybridization was conducted essentially as previously described (Gong et al., 2005) with minor modifications, as detailed in the supplementary Materials and Methods.

Subcellular localization analyses

Confocal microscopy was performed in transgenic seedlings, bombarded leek epidermal cells or agroinfiltrated *N. benthamiana* leaves using either a Leica TCS SP5 II or an Olympus FV1000.2.4 confocal microscope. For GFP activity of transgenic seedlings (35S:DRA2-GFP and 35S:NtDRA2-GFP lines) at least two independent transgenic lines were examined for each construct. Details of the constructs and the protocols used for the bombardments or the agroinfiltration are provided in the supplementary Materials and Methods.

Acknowledgements

We thank the CRAG greenhouse service for plant care; Chus Burillo for technical help; Sergi Portolés and Carles Rentero for assistance with mutagenesis; Mark Estelle (UCSD, USA) for providing *sar1-4*, *sar3-1* and *sar3-3* seeds; Juanjo López-Moya (CRAG, Barcelona; 35S:HoPro plasmid) and Dolores Ludevid (CRAG; C307 plasmid) for providing DNA plasmids; and Manuel Rodríguez-Concepción (CRAG) and Miguel Blázquez (IBMCP, Valencia, Spain) for comments on the manuscript.

Competing interests

The authors declare no competing or financial interests.

Author contributions

M.G., A.G., S.P., C.T., A.F.-A., L.L.-O., I.R.-V., X.W., J.L.M., M.R.P., P.F.D. and J.F.M.-G. performed experiments and data analyses; M.G., A.G., S.P., C.T., M.R.P. and J.F.M.-G. prepared the manuscript; and L.L.-O., I.R.-V., J.L.M. and P.F.D. contributed comments to the final version of the manuscript.

Funding

M.G. received an FPI fellowship from the Spanish Ministerio de Economía y Competitividad (MINECO). A.G. and A.F.-A. received FPU fellowships from the Spanish Ministerio de Educación. S.P. received an FI fellowship from the Agència de Gestió d'Ajuts Universitaris i de Recerca (AGAUR - Generalitat de Catalunya). C.T. received a Marie Curie IEF postdoctoral contract funded by the European Commission. I.R.-V. received initially an FPI fellowship from the Spanish MINECO and later a Beatriu de Pinós contract from AGAUR. Our research is supported by grants from the Spanish MINECO-FEDER [BIO2008-00169, BIO2011-23489 and BIO2014-59895-P] and Generalitat de Catalunya [2011-SGR447 and Xarba] to J.F.M.-G., and Generalitat Valenciana [PROMETEO/2009/112, PROMETEOII/2014/006] to M.R.P. and J.L.M. We acknowledge the support of the Spanish MINECO for the 'Centro de Excelencia Severo Ochoa 2016-2019' [award SEV-2015-0533].

Supplementary information

Supplementary information available online at
http://dev.biologists.org/lookup/suppl/doi:10.1242/dev.130211/-/DC1

References

- Bae, G. and Choi, G. (2008). Decoding of light signals by plant phytochromes and their interacting proteins. *Annu. Rev. Plant Biol.* **59**, 281–311.
- Bou-Torrent, J., Roig-Villanova, I., Galstyan, A. and Martínez-García, J. F. (2008). PAR1 and PAR2 integrate shade and hormone transcriptional networks. *Plant Signal. Behav.* **3**, 453–454.
- Bou-Torrent, J., Galstyan, A., Gallemí, M., Cifuentes-Esquivel, N., Molina-Contreras, M. J., Salla-Martret, M., Jikumaru, Y., Yamaguchi, S., Kamiya, Y. and Martínez-García, J. F. (2014). Plant proximity perception dynamically modulates hormone levels and sensitivity in Arabidopsis. *J. Exp. Bot.* **65**, 2937–2947.
- Bou-Torrent, J., Toledo-Ortiz, G., Ortiz-Alcaide, M., Cifuentes-Esquivel, N., Halliday, K. J., Martínez-García, J. F. and Rodríguez-Concepción, M. (2015). Regulation of carotenoid biosynthesis by shade relies on specific subsets of antagonistic transcription factors and cofactors. *Plant Physiol.* **169**, 1584–1594.
- Capelson, M. and Hetzer, M. W. (2009). The role of nuclear pores in gene regulation, development and disease. *EMBO Rep.* **10**, 697–705.
- Capelson, M., Liang, Y., Schulte, R., Mair, W., Wagner, U. and Hetzer, M. W. (2010). Chromatin-bound nuclear pore components regulate gene expression in higher eukaryotes. *Cell* **140**, 372–383.
- Cifuentes-Esquivel, N., Bou-Torrent, J., Galstyan, A., Gallemí, M., Sessa, G., Salla-Martret, M., Roig-Villanova, I., Ruberti, I. and Martínez-García, J. F. (2013). The bHLH proteins BEE and BIM positively modulate the shade avoidance syndrome in Arabidopsis seedlings. *Plant J.* **75**, 989–1002.
- Crocco, C. D., Holm, M., Yanovsky, M. J. and Botto, J. F. (2010). AtBBX21 and COP1 genetically interact in the regulation of shade avoidance. *Plant J.* **64**, 551–562.
- D'Angelo, M. A., Raices, M., Panowski, S. H. and Hetzer, M. W. (2009). Age-dependent deterioration of nuclear pore complexes causes a loss of nuclear integrity in postmitotic cells. *Cell* **136**, 284–295.
- Devlin, P. F., Yanovsky, M. J. and Kay, S. A. (2003). A genomic analysis of the shade avoidance response in Arabidopsis. *Plant Physiol.* **133**, 1617–1629.
- Dong, C.-H., Hu, X., Tang, W., Zheng, X., Kim, Y. S., Lee, B.-H. and Zhu, J.-K. (2006). A putative Arabidopsis nucleoporin, AtNUP160, is critical for RNA export and required for plant tolerance to cold stress. *Mol. Cell. Biol.* **26**, 9533–9543.
- Ferrandez-Ayela, A., Alonso-Peral, M. M., Sanchez-Garcia, A. B., Micol-Ponce, R., Perez-Perez, J. M., Micol, J. L. and Ponce, M. R. (2013). Arabidopsis TRANSCURVATA1 encodes NUP58, a component of the nucleopore central channel. *PLoS ONE* **8**, e67661.
- Fontoura, B. M. A., Blobel, G. and Yaseen, N. R. (2000). The nucleoporin Nup98 is a site for GDP/GTP exchange on ran and termination of karyopherin beta 2-mediated nuclear import. *J. Biol. Chem.* **275**, 31289–31296.
- Franklin, K. A. (2008). Shade avoidance. *New Phytol.* **179**, 930–944.
- Gangappa, S. N., Crocco, C. D., Johansson, H., Datta, S., Hettiarachchi, C., Holm, M. and Botto, J. F. (2013). The Arabidopsis B-BOX protein BBX25 interacts with HY5, negatively regulating BBX22 expression to suppress seedling photomorphogenesis. *Plant Cell* **25**, 1243–1257.
- Gong, Z., Dong, C.-H., Lee, H., Xiong, L., Gong, D., Stevenson, B. and Zhu, J. K. (2005). A DEAD box RNA helicase is essential for mRNA export and important for development and stress responses in Arabidopsis. *Plant Cell* **17**, 256–267.
- Griffis, E. R., Altan, N., Lippincott-Schwartz, J. and Powers, M. A. (2002). Nup98 is a mobile nucleoporin with transcription-dependent dynamics. *Mol. Biol. Cell* **13**, 1282–1297.
- Hodel, A. E., Hodel, M. R., Griffis, E. R., Hennig, K. A., Ratner, G. A., Xu, S. and Powers, M. A. (2002). The three-dimensional structure of the autophosphorylated, nuclear pore-targeting domain of the human nucleoporin Nup98. *Mol. Cell* **10**, 347–358.

- Jacob, Y., Mongkolsiriwatana, C., Velez, K. M., Kim, S. Y. and Michaels, S. D. (2007). The nuclear pore protein AtTPR is required for RNA homeostasis, flowering time, and auxin signaling. *Plant Physiol.* **144**, 1383–1390.
- Josse, E.-M., Foreman, J. and Halliday, K. J. (2008). Paths through the phytochrome network. *Plant Cell Environ.* **31**, 667–678.
- Kalverda, B., Pickersgill, H., Shloma, V. V. and Fornerod, M. (2010). Nucleoporins directly stimulate expression of developmental and cell-cycle genes inside the nucleoplasm. *Cell* **140**, 360–371.
- Keuskamp, D. H., Sasidharan, R. and Pierik, R. (2010). Physiological regulation and functional significance of shade avoidance responses to neighbors. *Plant Signal. Behav.* **5**, 655–662.
- Kozma Bogнар, L., Hall, A., Adam, E., Thain, S. C., Nagy, F. and Millar, A. J. (1999). The circadian clock controls the expression pattern of the circadian input photoreceptor, phytochrome B. *Proc. Natl. Acad. Sci. USA* **96**, 14652–14657.
- Leivar, P. and Quail, P. H. (2011). PIFs: pivotal components in a cellular signaling hub. *Trends Plant Sci.* **16**, 19–28.
- Li, L., Ljung, K., Breton, G., Schmitz, R. J., Pruneda-Paz, J., Cowing-Zitron, C., Cole, B. J., Ivans, L. J., Pedmale, U. V., Jung, H.-S. et al. (2012). Linking photoreceptor excitation to changes in plant architecture. *Genes Dev.* **26**, 785–790.
- Liang, Y., Franks, T. M., Marchetto, M. C., Gage, F. H. and Hetzer, M. W. (2013). Dynamic association of NUP98 with the human genome. *PLoS Genet.* **9**, e1003308.
- Light, W. H., Freaney, J., Sood, V., Thompson, A., D'Urso, A., Horvath, C. M. and Brickner, J. H. (2013). A conserved role for human Nup98 in altering chromatin structure and promoting epigenetic transcriptional memory. *PLoS Biol.* **11**, e1001524.
- Lorrain, S., Allen, T., Duek, P. D., Whitelam, G. C. and Fankhauser, C. (2008). Phytochrome-mediated inhibition of shade avoidance involves degradation of growth-promoting bHLH transcription factors. *Plant J.* **53**, 312–323.
- MacGregor, D. R., Gould, P., Foreman, J., Griffiths, J., Bird, S., Page, R., Stewart, K., Steel, G., Young, J., Paszkiewicz, K. et al. (2013). HIGH EXPRESSION OF OSMOTICALLY RESPONSIVE GENES1 is required for circadian periodicity through the promotion of nucleocytoplasmic mRNA export in Arabidopsis. *Plant Cell* **25**, 4391–4404.
- Martínez-García, J. F., Huq, E. and Quail, P. H. (2000). Direct targeting of light signals to a promoter element-bound transcription factor. *Science* **288**, 859–863.
- Martínez-García, J. F., Virgos-Soler, A. and Prat, S. (2002). Control of photoperiod-regulated tuberization in potato by the Arabidopsis flowering-time gene CONSTANS. *Proc. Natl. Acad. Sci. USA* **99**, 15211–15216.
- Martínez-García, J. F., Galstyan, A., Salla-Martret, M., Cifuentes-Esquivel, N., Gallemí, M. and Bou-Torrent, J. (2010). Regulatory components of shade avoidance syndrome. *Adv. Bot. Res.* **53**, 65–116.
- Martínez-García, J. F., Gallemí, M., Molina-Contreras, M. J., Llorente, B., Bevilacqua, M. R. R. and Quail, P. H. (2014). The shade avoidance syndrome in Arabidopsis: the antagonistic role of phytochrome A and B differentiates vegetation proximity and canopy shade. *PLoS ONE* **9**, e109275.
- Parry, G. (2013). Assessing the function of the plant nuclear pore complex and the search for specificity. *J. Exp. Bot.* **64**, 833–845.
- Parry, G. (2014). Components of the Arabidopsis nuclear pore complex play multiple diverse roles in control of plant growth. *J. Exp. Bot.* **65**, 6057–6067.
- Parry, G., Ward, S., Cernac, A., Dharmasiri, S. and Estelle, M. (2006). The Arabidopsis SUPPRESSOR OF AUXIN RESISTANCE proteins are nucleoporins with an important role in hormone signaling and development. *Plant Cell* **18**, 1590–1603.
- Powers, M. A., Forbes, D. J., Dahlberg, J. E. and Lund, E. (1997). The vertebrate GLFG nucleoporin, Nup98, is an essential component of multiple RNA export pathways. *J. Cell Biol.* **136**, 241–250.
- Radu, A., Moore, M. S. and Blobel, G. (1995). The peptide repeat domain of nucleoporin Nup98 functions as a docking site in transport across the nuclear pore complex. *Cell* **81**, 215–222.
- Raices, M. and D'Angelo, M. A. (2012). Nuclear pore complex composition: a new regulator of tissue-specific and developmental functions. *Nat. Rev. Mol. Cell Biol.* **13**, 687–699.
- Roig-Villanova, I., Bou, J., Sorin, C., Devlin, P. F. and Martínez-García, J. F. (2006). Identification of primary target genes of phytochrome signaling. Early transcriptional control during shade avoidance responses in Arabidopsis. *Plant Physiol.* **141**, 85–96.
- Roig-Villanova, I., Bou-Torrent, J., Galstyan, A., Carretero-Paulet, L., Portolés, S., Rodríguez-Concepción, M. and Martínez-García, J. F. (2007). Interaction of shade avoidance and auxin responses: a role for two novel atypical bHLH proteins. *EMBO J.* **26**, 4756–4767.
- Salter, M. G., Franklin, K. A. and Whitelam, G. C. (2003). Gating of the rapid shade-avoidance response by the circadian clock in plants. *Nature* **426**, 680–683.
- Sessa, G., Carabelli, M., Sassi, M., Ciolfi, A., Possenti, M., Mitterperger, F., Becker, J., Morelli, G. and Ruberti, I. (2005). A dynamic balance between gene activation and repression regulates the shade avoidance response in Arabidopsis. *Genes Dev.* **19**, 2811–2815.
- Singer, S., Zhao, R., Barsotti, A. M., Ouwehand, A., Fazollahi, M., Coutavas, E., Breuhahn, K., Neumann, O., Longrich, T., Pusterla, T. et al. (2012). Nuclear pore component Nup98 is a potential tumor suppressor and regulates posttranscriptional expression of select p53 target genes. *Mol. Cell* **48**, 799–810.
- Smith, H. (1982). Light quality, photoperception, and plant strategy. *Annu. Rev. Plant Physiol.* **33**, 481–518.
- Smith, H. and Whitelam, G. C. (1997). The shade avoidance syndrome: multiple responses mediated by multiple phytochromes. *Plant Cell Environ.* **20**, 840–844.
- Sorin, C., Salla-Martret, M., Bou-Torrent, J., Roig-Villanova, I. and Martínez-García, J. F. (2009). ATHB4, a regulator of shade avoidance, modulates hormone response in Arabidopsis seedlings. *Plant J.* **59**, 266–277.
- Tamura, K. and Hara-Nishimura, I. (2013). The molecular architecture of the plant nuclear pore complex. *J. Exp. Bot.* **64**, 823–832.
- Tamura, K., Fukao, Y., Iwamoto, M., Haraguchi, T. and Hara-Nishimura, I. (2011). Identification and characterization of nuclear pore complex components in Arabidopsis thaliana. *Plant Cell* **22**, 4084–4097.
- Wang, X., Roig-Villanova, I., Khan, S., Shanahan, H., Quail, P. H., Martínez-García, J. F. and Devlin, P. F. (2011). A novel high-throughput in vivo molecular screen for shade avoidance mutants identifies a novel phyA mutation. *J. Exp. Bot.* **62**, 2973–2987.
- Xu, X. M. and Meier, I. (2008). The nuclear pore comes to the fore. *Trends Plant Sci.* **13**, 20–27.
- Xu, X. M., Meulia, T. and Meier, I. (2007). Anchorage of plant RanGAP to the nuclear envelope involves novel nuclear-pore-associated proteins. *Curr. Biol.* **17**, 1157–1163.
- Zhao, Q. and Meier, I. (2011). Identification and characterization of the Arabidopsis FG-repeat nucleoporin Nup62. *Plant Signal. Behav.* **6**, 330–334.